Chemical Engineering Journal 375 (2019) 122070

Contents lists available at ScienceDirect

Chemical Engineering Journal

journal homepage: www.elsevier.com/locate/cej

Activation of persulfate by photoexcited dye for antibiotic degradation: Radical and nonradical reactions

Tao Cai[a,b], Yutang Liu[a,b,*], Longlu Wang[c], Wanyue Dong[a,b], Hui Chen[a,b], Wengao Zeng[a,b], Xinnian Xia[d], Guangming Zeng[a,b]

[a] College of Environmental Science and Engineering, Hunan University, Lushan South Road, Yuelu District, Changsha 410082, PR China
[b] Key Laboratory of Environmental Biology and Pollution Control (Hunan University), Ministry of Education, Lushan South Road, Yuelu District, Changsha 410082, PR China
[c] School of Physics and Electronics, Hunan University, Changsha 410082, PR China
[d] College of Chemistry and Chemical Engineering, Hunan University, Changsha 410082, PR China

HIGHLIGHTS

- TC-H, 2,4-DNP and NOMs can be efficiently degraded by dye- activated PS.
- Both radical and nonradical reactions were discovered in Dye/PS/Vis system.
- LUMO levels of dyes have great influence on PS activation.
- Phenolic intermediates of dye degradation play an important role in PS activation.
- Effects of dye type, dye dose, DO and pH on PS activation were identified.

GRAPHICAL ABSTRACT

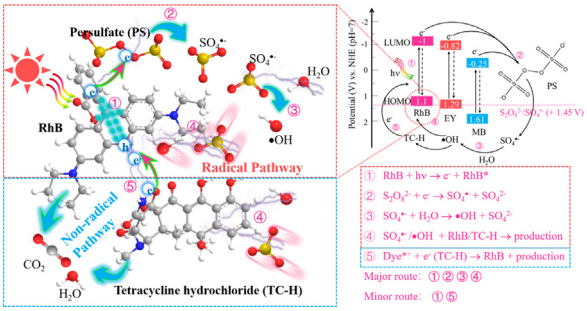

ARTICLE INFO

Keywords:
Persulfate
Antibiotic
Dye
Radical reaction
Nonradical reaction

ABSTRACT

Despite numerous studies on peroxydisulfate (PS) activation with catalysts, the PS activation by organic contaminants themselves has been rarely reported. Here, we found that PS can be activated by dyes such as rhodamine B (RhB), eosin Y (EY) and methylene blue (MB) under visible light (Vis) irradiation, achieving simultaneous degradation of dye and antibiotics (e.g., tetracycline hydrochloride) via both radical and nonradical pathways. Experimental results demonstrated that the radical reaction was the major route, which was caused by the reduction of PS by photogenerated electrons of the dye. Dye-mediated electron transfer from pollutants to the oxidized dye (dye^{*+}) was responsible for the nonradical reaction. Compared with EY and MB, the most negative LUMO (lowest unoccupied molecular orbital) level of RhB facilitated rapid electron transfer from RhB to PS, resulting in the highest activation efficiency. Interestingly, post-processing with base can further increase the mineralization efficiency due to the PS activation by generated phenolic intermediates of RhB degradation. This work elucidated a new pathway of PS activation and provide a new "using waste to treat waste" strategy for the disposal of dye wastewater and complex wastewater containing dye.

* Corresponding author at: College of Environmental Science and Engineering, Hunan University, Lushan South Road, Yuelu District, Changsha 410082, PR China.
E-mail address: yt_liu@hnu.edu.cn (Y. Liu).

https://doi.org/10.1016/j.cej.2019.122070
Received 15 April 2019; Received in revised form 20 June 2019; Accepted 23 June 2019
Available online 24 June 2019
1385-8947/ © 2019 Elsevier B.V. All rights reserved.

1. Introduction

Organic pollutant such as antibiotics has caused a serious risk to aquatic environment and human health [1]. Advanced oxidation processes (AOPs) based on peroxydisulfate (PS) and peroxomonosulfate (PMS) have been extensively applied for environmental remediation. PS is almost non-hygroscopic and has a good stability and it is cheap in comparison to other oxidants such as PMS [2]. The bond dissociation energy and bond length of $[O_3SO\text{-}OSO_3]^{2-}$ were determined to be 140 kJ mol^{-1} and 1.497 Å, respectively [3]. It can be activated to generate highly reactive sulfate radicals ($SO_4^{\cdot -}$) and hydroxyl radicals (·OH) [4,5]. These radicals can degrade a wide range of environmental pollutants, such as polycyclic aromatic hydrocarbons and numerous volatile organic compounds [6]. Transition metal ions, [7,8] oxides, [9,10] carbon materials, [3,11] and energy (e.g., heat [12] and ultraviolet [13,14]) are usually used to activate PS or PMS, and the associated activation mechanisms have been well studied.

In addition to these activation methods, recent studies showed that PS and PMS can also be activated by some organic compounds. For example, Fang et al. [6] reported that PS can be activated by benzoquinone via a semiquinone radical-dependent Fenton-like reaction. Zhou et al. [15] found that PMS also can be activated by benzoquinone but followed a novel nonradical oxidation mechanism, where the production of $^1O_2$ was involved. The anionic form of phenols can activate PS via a one-electron reduction mechanism ($PhO^- + S_2O_8^{2-} \rightarrow SO_4^{2-} + SO_4^{\cdot -} + PhO_{ox}$, Eq. (1)), which reported by Ahmad et al. [16]. Interestingly, Zhou et al. [17] revealed the mechanism of PMS activation by phenols was attributed to the singlet oxygenation. It should be mentioned that in contrast to benzoquinone and phenols, PS activation by other organics is not well understood. Investigation of the interaction between organics and PS could facilitate the understanding of AOPs and develop effective and economically feasible environmental remediation strategies.

A large amount of dye wastewater is discharged without effective treatment, which has been one of the major environmental pollution issues [18]. Due to the complicated molecular structure, there is a recalcitrance to degradation in conventional wastewater treatment processes [19]. If PS can be activated by dyes, it would alleviate the burden of dye wastewater disposal and save costs because no additional activator would be needed. It also might be applied to treat complex wastewater containing dyes to achieve “using waste to treat waste” strategy. Actually, dyes are widely applied in dye-sensitized solar cells, where charge separation occurs at the dye-semiconductor interface via photoexcited process [20,21]. In this regard, photoexcited electrons might be utilized to reduce PS to produce $SO_4^{\cdot -}$ and oxidized dye (dye^{*+}) might directly oxidize target pollutant through electron abstraction. However, these processes and mechanisms have been poorly investigated so far.

Gao et al. [22] reported that the excited Rhodamine B (RhB*) and the Fe(II) species formed on the surface of clay/iron-based catalyst can effectively activate PS to produce radicals. However, they only focused on the production of radicals and the cycling of Fe(II) and Fe(III) species while the mechanism of dye-activated PS and its oxidation behavior have not been examined in much detail. To date, the application and understanding of photoexcited dye–activated PS are very limited and involve the following shortcomings: (i) mechanistic insight into the Dye/PS/Vis system is very weak and limited to radical reaction; (ii) how the molecular structure of dyes affects the PS activation has not been reported; (iii) little is known about the effect of intermediates produced during dye degradation on PS activation; (iv) the use of dye as PS activators to degrade other pollutants remain elusive.

In this work, RhB, methylene blue (MB) and eosin Y (EY) as cationic dyes with different lowest unoccupied molecular orbital (LUMO) level were selected to investigate the effects of level structure on PS activation. Methyl orange (MO), an anionic dye, also selected as activator to study the effects of charged type of dye on PS activation. Tetracycline hydrochloride (TC-H) and 2,4-Dinitrophenol (2,4-DNP) were employed as model contaminants. The PS activation process and mechanism by photoexcited dye were probed. It was investigated how the type of dye and other possible factors (e.g., dissolved oxygen (DO), PS concentration, dye dose and initial pH) affected PS activation efficiency. Moreover, The effects of phenolic intermediates from RhB degradation on the PS activation under basic conditions were also studied. This work revealed that dyes could be used as the PS activators to effectively remove environmental pollutants from simulated wastewater.

2. Experimental section

2.1. Chemicals

All chemicals used in this work were described in Supplementary information (SI Text S1).

2.2. Experiments

2.2.1. PS activation by photoexcited dye

The activation experiment was performed in a 50 mL quartz reactor (SI Fig. S1) at room temperature without using circulating cooling water. A 300 W Xe lamp with a cut-off filter ($\lambda > 420$ nm) as the light source. Reaction systems consisted of 0.65 mM potassium peroxydisulfate ($K_2S_2O_8$) and 10 mg/L dye such as RhB, MB and EY, which were named RhB/PS/Vis, MB/PS/Vis and EY/PS/Vis system, respectively. During the reaction, 1 mL of reaction liquid was taken out at a given interval time for further analysis.

2.2.2. Pollutants degradation by photoexcited dye-activated PS

RhB/PS/Vis system was employed as the model system to investigate the degradation of pollutants by dye-activated PS. Reaction systems consisted of 0.65 mM $K_2S_2O_8$, 10 mg/L RhB and 10 mg/L pollutants (TC-H or 2,4-DNP). A 300 W Xe lamp with a cut-off filter ($\lambda > 420$ nm) as the light source. During the reaction, 1 mL of reaction liquid was taken out at a given interval time for further analysis.

2.2.3. Radical detection

The generation of radicals was detected by electron paramagnetic resonance (EPR) and the fluorescence emission of 7-hydroxycoumarin (7-HC). EPR detection was carried out on a JES FA200 electron paramagnetic resonance spectrometer. Experiments were carried out in a mixed solution of 10 mg/L RhB dye, 0.65 mM PS and 20 mM 5,5-dimethyl-1-pyrrolidine N-oxide (DMPO) under visible light irradiation (SI Text S2). Additionally, the generation of ·OH can also be indirectly detected by the fluorescence emission of 7-HC (SI Text S3).

2.3. Analytical methods

The concentrations of RhB, MB, EY, MO, TC-H, and 2,4-DNP were measured by optical absorption at 554 nm, 664 nm, 517 nm, 465 nm, 357 nm and 370 nm, respectively, with a UV–vis spectrophotometer (CARY 300 Conc).

To probe the effects of intermediates of RhB degradation on PS activation, high-performance liquid chromatography/mass spectrometry (HPLC-MS, Agilent Technology 1290/6460 Triple Quad LC/MS) with electron spray ionization (ESI) positive mode was used to detect the degradation intermediates. The samples were chromatographically separated using a ZORBAX Eclipse Plus C18 (2.1 × 50 mm and 1.8-mm) at a flow rate of 0.2 mL min^{-1}. The mobile phase was methanol and water (60:40, v/v).

PS concentrations were determined by potassium iodide method [6]. (SI Text S4). Luminous power was recorded by photometer (PM-MW 2000, S = 3.14 cm^2). pH tested by a pH meter (FE28, Mettler Toledo). The fluorescence emission of RhB was measured by Hitachi F-7000 fluorescence spectrophotometer (SI Text S5). Total organic carbon

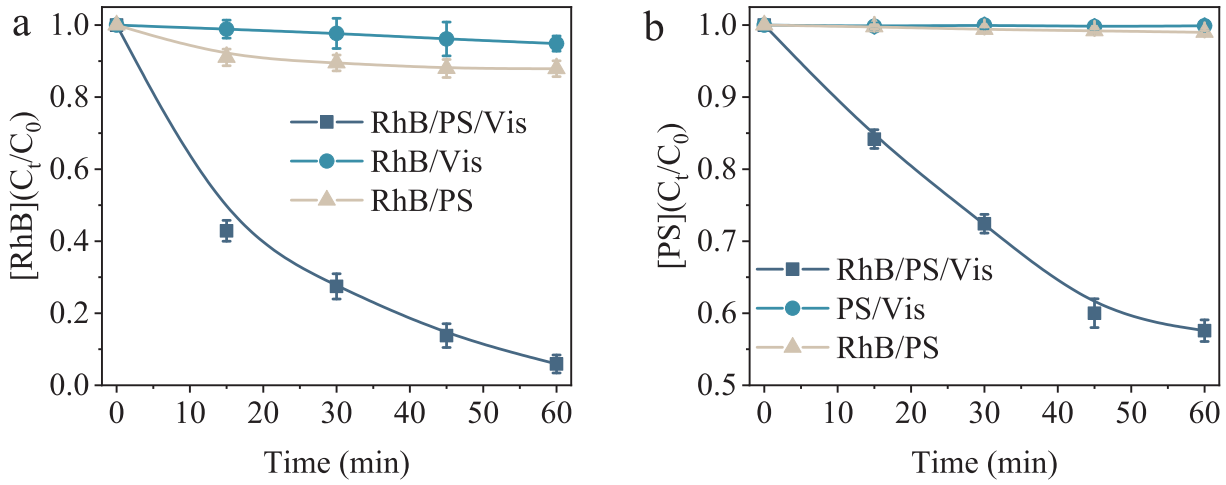

Fig. 1. The activation of PS and degradation of RhB in RhB/PS/Vis system. (a), degradation of RhB by PS, Vis or PS/Vis; (b), decomposition of PS by RhB, Vis or RhB/Vis. The experimental conditions: [RhB] = 10 mg/L, [PS] = 0.65 mM, and λ > 420 nm irradiation.

(TOC) were tested by a TOC analyzer (TOC-VCPH/CPN, Shimadzu).

3. Results and discussion

3.1. Dye degradation and PS activation

Fig. 1a showed the results of degradation of 10 mg/L RhB by 0.65 mM PS with and without visible light. As can be seen, 94.1% of RhB was degraded by PS under visible light illumination (RhB/PS/Vis), while separately only 5.1% or 12.1% of RhB was degraded by visible light or PS. This results indicated that the degradation of RhB by PS was greatly enhanced under visible light irradiation. To check whether the increased degradation efficiency was due to the PS activation, the variation of PS concentration was monitored during reaction process. As shown in Fig. 1b, 43.5% of PS was decomposed in RhB/PS/Vis system, while almost no change in the PS concentration in RhB/PS or PS/Vis system can be observed. The result indicated that neither RhB nor visible light can activate PS, and it can only be activated when both RhB and visible light existed. Based on above experimental results and deduction, a preliminary conclusion can be obtained that RhB can activate PS under visible light illumination and exhibit autocatalytic degradation.

Since Edwards first reported the cobaltous-mediated activation of persulfate, there have been many works study the mechanisms of this process [23]. As we know, PS can also be activated by heat [12]. To differentiate the contributions of photoexcited effects and photothermal effects in our research, the PS activation by heat was studied (PS/heat). Fig. S2a showed the variation of reaction temperature in RhB/PS/Vis system within the time scale. As the reaction progresses, the temperature of the system raised from 22 °C to 50 °C within 60 min. For simplicity, RhB/PS/heat process was performed at a constant temperature of 50 °C for 60 min. As shown in Fig. S2b, the degradation of RhB was negligible, implying that the photothermal effects played a weak role on PS activation under our experimental conditions.

To further demonstrate that PS activation was caused by photoexcited effects of dye, the activation experiment was carried out under monochromatic light irradiation. The maximum absorption peak of RhB is at 550 nm, but its absorption at 450 nm is relatively weak (SI Fig. S3a). If the PS activation arises from photoexcited RhB, under different monochromatic light wavelengths irradiation the decomposition efficiency of RhB and PS at 550 nm will be significantly higher than that at 450 nm. Unsurprisingly, 72.2% of RhB and 7% PS were decomposed within 120 min under 550 nm monochromatic light irradiation, while only 40.8% of RhB and 2.5% of PS were decomposed under 450 nm monochromatic light illumination (SI Fig. S3b, c). The above results demonstrated that the PS activation was caused by the photoexcited RhB. In sum, we can conclude that RhB shows autocatalysis under visible light irradiation due to the PS activation by RhB itself.

3.2. Mechanism of PS activation by photoexcited dye

In the dye-sensitized solar cells system, the photochemical reactions are initiated via the electron injection from the excited state dye (dye*) into the conduction band of the semiconductor [20]. PS activation by photoexcited dye might follow a similar electron-mediated reduction mechanism. To probe the possible mechanism, the fluorescence emission intensity of RhB solution in the presence or absence of PS was monitored. The magnitude of the fluorescence intensity usually reflects the level of charge separation efficiency [24]. Therefore, efficient electron transfer from RhB* to PS will greatly reduce its fluorescence intensity. Fig. 2a showed that the fluorescence intensities were obviously decreased when PS was added to RhB solution. Additionally, the concentration of RhB did not change before and after the measurement (SI Fig. S4), indicating that the decrease in fluorescence intensity was caused by electron transfer from RhB* to PS but not the degradation of RhB. Thus, RhB-induced PS activation and autocatalysis degradation process may involve following steps (Eqs. (2)–(5)). Firstly, RhB absorbed light to produce photoexcited electrons and oxidized RhB (RhB^{*+}) (Eq. (2)); Then, PS reduced by photoexcited electrons to produce $SO_4^{\cdot -}$ and ·OH (Eqs. (3) and (4)); Finally, the produced radicals attacked RhB molecule and caused its degradation (Eq. (5)).

$$RhB + h\nu \rightarrow e^- + RhB^{*+} \quad (2)$$

$$S_2O_8^{2-} + e^- \rightarrow SO_4^{\cdot -} + SO_4^{2-} \quad (3)$$

$$SO_4^{\cdot -} + OH^- \rightarrow SO_4^{2-} + \cdot OH \quad (4)$$

$$SO_4^{\cdot -}/\cdot OH + RhB \rightarrow products \quad (5)$$

The generation of ·OH can be detected by the fluorescence signal of 7-hydroxycoumarin (7-HC) (SI Fig. S5), which is produced from the reaction between the ·OH and coumarin [25]. For the PS activation process, we monitored the variation of the PS concentration and 7-HC signal intensity in RhB/PS/Vis system (Fig. 2b). We found that PS concentration decreased from 0.65 mM to 0.34 mM within 60 min, while corresponding the 7-HC signal intensity increased rapidly. This result is consistent with the above mechanism (Eqs. (3) and (4)), where PS decomposition was responsible for radical generation. Reactive oxygen species (ROSs) quenching experiments confirmed that $SO_4^{\cdot -}$ and ·OH were main ROSs (Fig. 2c), in which *tert*-butanol (TBA) and ethanol (EtOH) were employed as the sacrificial agent for ·OH and

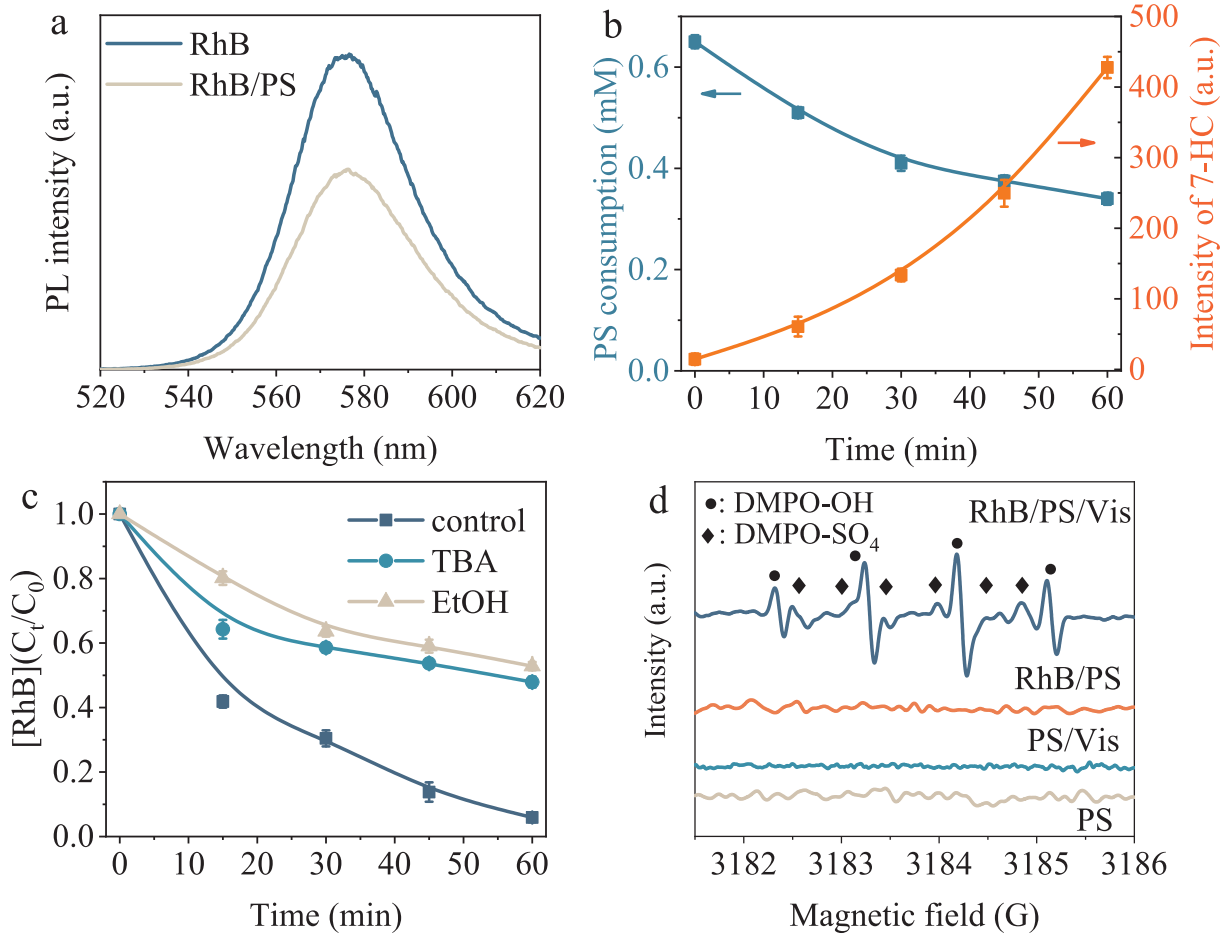

Fig. 2. Activation of PS by photoexcited RhB and the generation of $SO_4^{\cdot -}$ and ·OH. (a), the fluorescence emission intensity of RhB with and without PS; (b), the relationship of the decomposition of PS and the generation of ·OH; (c), Effect of scavengers on RhB degradation in RhB/PS/Vis system; (d), EPR spectra of PS, RhB/PS and RhB/PS/Vis system. Experimental conditions for (a): [PS] = 1 mM and [RhB] = 10 mg/L; (b): [PS] = 0.65 mM, [RhB] = 10 mg/L and [coumarin] = 1 mM; (c): [PS] = 0.65 mM, [RhB] = 10 mg/L and [TBA] = [EtOH] = 0.2 M; (d): [PS] = 0.65 mM, [RhB] = 10 mg/L, [DMPO] = 20 mM, and reaction time of 10 min.

$SO_4^{\cdot -}$/·OH, respectively [4,26]. 5,5-dimethyl pyrroline-oxide (DMPO) was used as the spin trapping reagent to directly detect the production of $SO_4^{\cdot -}$ and ·OH [27,28]. EPR signals corresponding to DMPO-$SO_4^{\cdot -}$ and DMPO-·OH appeared in RhB/PS/Vis system (Fig. 2d), indicating that both $SO_4^{\cdot -}$ and ·OH were generated. However, no EPR signals can be observed in PS, RhB/PS and PS/Vis system, indicating no radical production. This result confirmed that photoexcited dye plays an important role in PS activation. All experimental results further support the above mechanism discussion (Eqs. (2)–(5)).

To further demonstrated that the PS activation arose from the PS reduction by photogenerated electrons of the dye, competing reactions between PS and $KBrO_3$ were carried out. $KBrO_3$ as an electron sacrificial agent [29] couldn't generate ·OH under visible light irradiation and degrade RhB (SI Fig. S6a, b). Interestingly, the degradation of RhB, the decomposition of PS and the generation of ·OH were greatly inhibited when $KBrO_3$ added into RhB/PS/Vis system (SI Fig. S7a, b). This is because $KBrO_3$ consumes a part of electrons and thus suppresses the reduction of PS. Therefore, the PS activation can be classified to the reduction mechanism induced by photogenerated electrons of dye.

To achieve efficient electron injection from dye to PS, the lowest unoccupied molecular orbital (LUMO) level of dyes should be more negative than the redox potential of PS ($S_2O_8^{2-}/SO_4^{\cdot -}$ (+1.45 V vs NHE) [30]) [20]. The LUMO level of RhB, EY and MB were −1.0 V, −0.82 V and −0.25 V vs NHE, respectively, which were obtained by calculation of density functional theory (DFT) in our previous work [31]. Interestingly, the PS decomposition efficiency was in the order of RhB > EY > MB in Dye/PS/Vis system (Fig. 3a), which matches well with the LUMO level of dye. The highest PS decomposition efficiency achieved in RhB/PS/Vis system was mainly attributed to the most negative LUMO level of RhB. Because organic molecules with more negative LUMO levels are more likely to donate electrons to electron acceptor [31]. Note that dye degradation does not follow the order of LUMO levels. This may be related to the structural stability of the dye itself. Based on the above discussion, we propose the mechanism of PS activation by dye and showed in Fig. 3b. Under light irradiation, electrons can be excited from the highest occupied molecular orbital (HOMO) to the LUMO of the dye, and then photogenerated electron will injected into PS molecule from the LUMO of the dye. Finally, the PS reduced by photogenerated electron and decomposed into $SO_4^{\cdot -}$.

3.3. Effects of dye type, DO, dye dose, and pH

3.3.1. Effects of dye type

To explore the effects of different dye types on PS activation, MO, anionic dye[32], was used as PS activator and compared with above cationic dyes. As shown in Fig. S8, 51% of 10 mg/L MO was degraded and 12.5% of 0.65 mM PS was decomposed in MO/PS/Vis system, which was significantly lower than the degradation and activation efficiency of those cationic dyes (Fig. 3a). The reason may be due to the electrostatic repulsion of anionic dyes with $S_2O_8^{2-}$, where electron transfer from MO to PS was hindered, resulting in lower activation efficiencies.

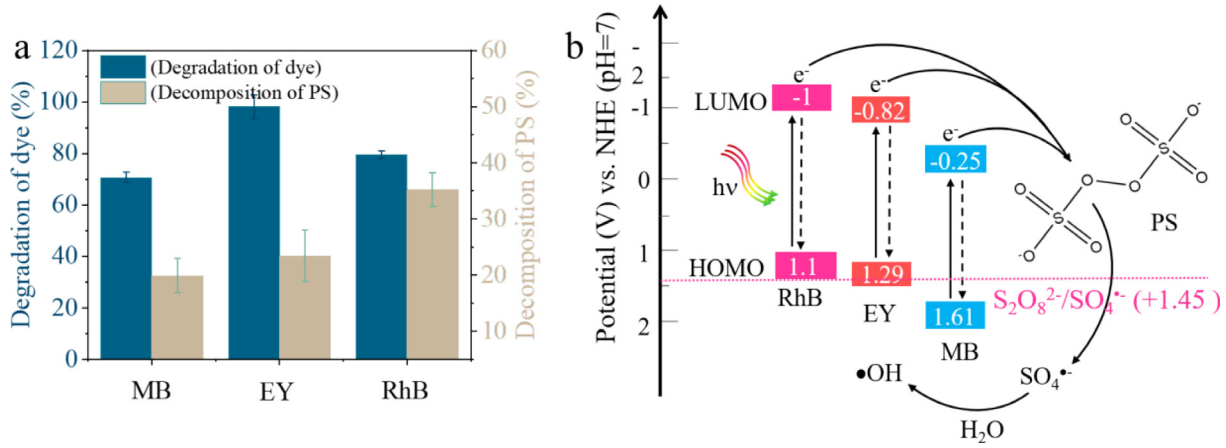

Fig. 3. The activation of PS by different dye and corresponding activation mechanism. (a), activation of PS in Dye/PS/Vis system; (b), mechanism of PS activation by dye under visible light irradiation. Experimental conditions: [PS] = 0.65 mM, [RhB] = [EY] = [MB] = 10 mg/L, reaction time of 60 min, and λ > 420 nm irradiation.

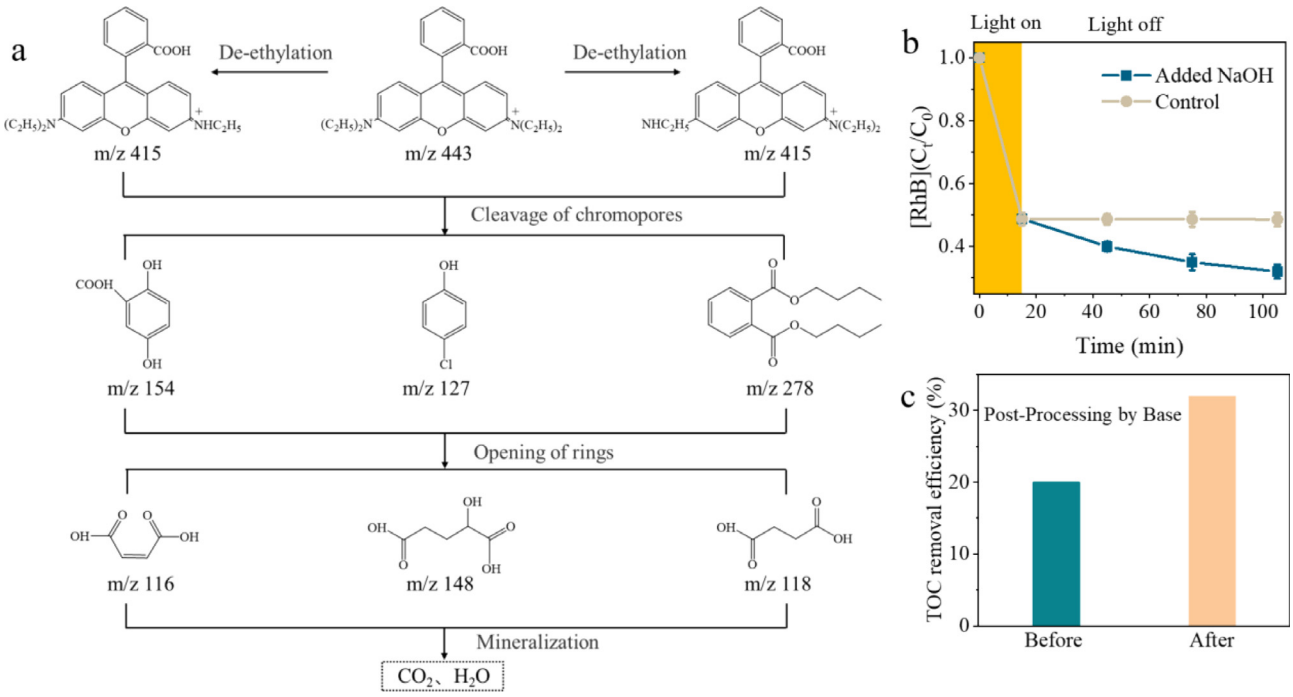

Fig. 4. Effects of intermediates on the PS activation. (a), the degradation pathway of RhB in RhB/PS/Vis; (b), effects of degradation intermediates of RhB on the PS activation; (c), TOC removal efficiency before and after treatment by base. Experimental conditions for (b): [PS] = 0.65 mM, [RhB] = 10 mg/L, and pH = 12 (Adjust pH with NaOH); (c): [PS] = 0.65 mM, [RhB] = 10 mg/L, photoreaction time was 60 min and time of post-processing with base (pH = 12) was 120 min.

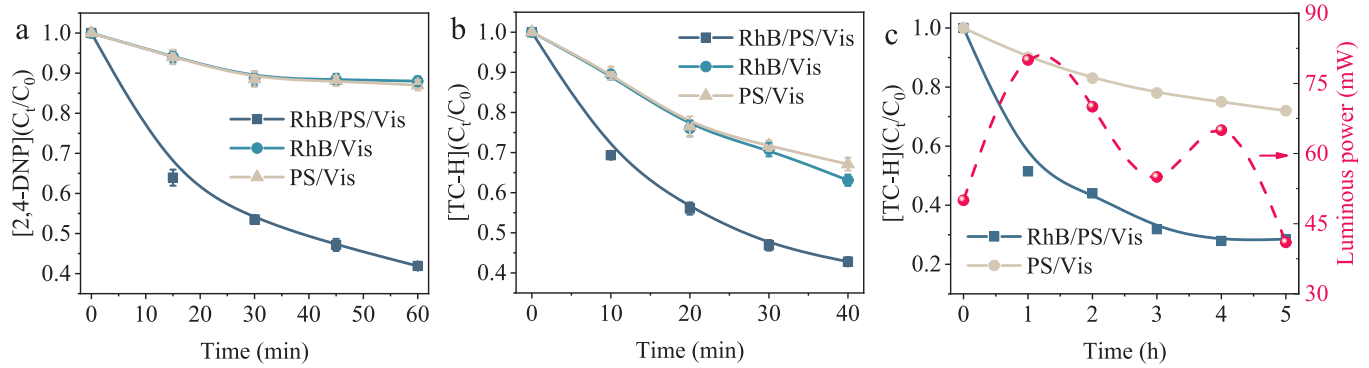

Fig. 5. The degradation of organic pollutants by photoexcited RhB/PS system. Time profiles of the degradation of (a) 2,4-DNP and (b) TC-H in RhB/PS/Vis system; (c), The degradation of TC-H in RhB/PS/Sunlight system. Experimental conditions: [PS] = 0.65 mM, [RhB] = 10 mg/L, and [2,4-DNP] = [TC-H] = 10 mg/L.

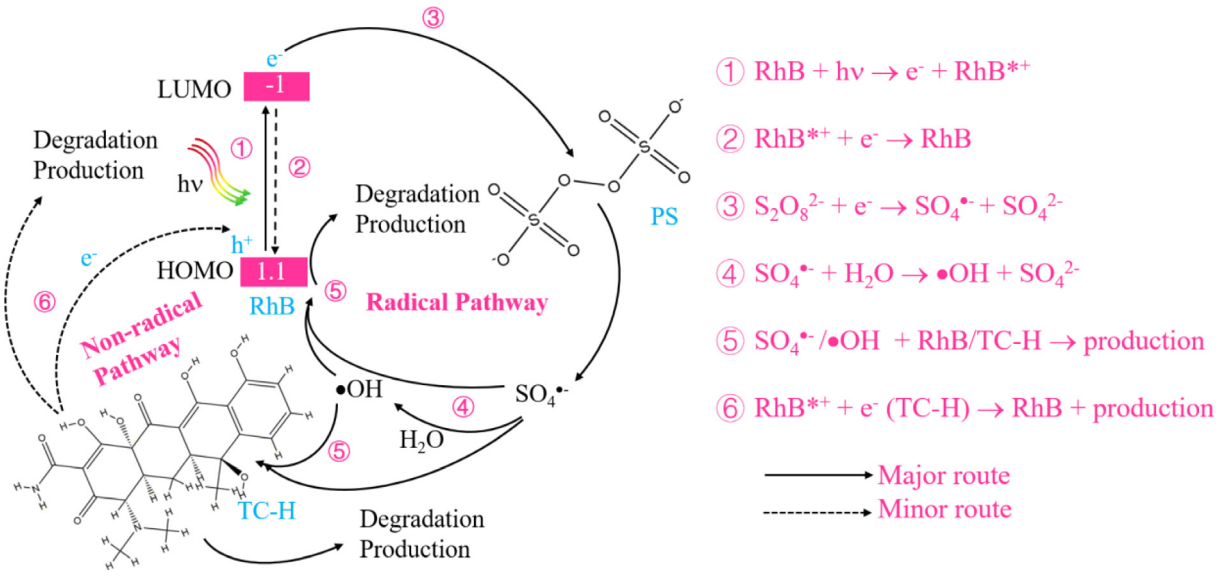

Fig. 6. The mechanism of TC-H degradation in RhB/PS/Vis system.

3.3.2. Effects of DO

Effects of DO on PS activation was also studied. Note that the decomposition efficiency of RhB and PS did not have an obvious change in the absence or presence of DO (SI Fig. S9a, b). In addition, the signal of ·OH generation was almost identical in oxic and anoxic system (SI Fig. S9c). It can conclude that DO plays a negligible role in the PS activation.

3.3.3. Effects of dye dose

Effects of dye dose on PS activation was displayed in Fig. S10. Fig. S10a showed the decomposition of PS by RhB of different concentrations. Obviously, the decomposition efficiency increased with the increase of RhB concentration. The plot of apparent rate constant (k_{obs}, pseudo-first-order approximation) vs [RhB] resulted in a straight line (SI Fig. S10b), indicating that the decomposition efficiency of PS was first-order with respect to [RhB]. The degradation efficiency of RhB was also first-order with respect to [PS] (SI Fig. S11a, b). Similarly, the decomposition efficiency of PS by other dyes (MB, EY and MO) increased with the increase of their concentration and followed pseudo-first-order model (SI Fig. S12).

3.3.4. Effects of pH

Effects of pH on PS activation was also investigated. The reaction of PS with RhB were carried out at various pH values and the k_{obs} for PS decomposition at each pH was calculated (SI Fig. S13a, b). Fig. S13c showed that the RhB degradation was inhibited as the pH values increased from 3 to 9. RhB exists in two main forms in aqueous media, namely, cationic (RhB^+) or in zwitterionic form ($RhB^{\pm}$). When the pH is lower than its pKa (3.7), it exists in the form of cationic. Nevertheless, when the pH values higher than its pKa, it exists in the form of zwitterionic because of the deprotonation of its carboxyl group [33]. Therefore, RhB was deprotonated at pH 9, [24] the weaker electrostatic attraction between RhB and PS would be detrimental to RhB degradation. Additionally, Fig. S14 showed the stepwise reaction mechanism for activation of PS under acidic and alkaline medium in presence of different dyes.

3.4. Post-processing by base: PS activation by phenolic intermediates of RhB degradation

Since PS activation was caused by photoexcited dyes, the activation would cease once RhB was completely bleached. Considering the complexity of the structure of RhB, the effects of intermediate products on PS activation was studied. The intermediate products of RhB degradation in RhB/PS/Vis system was detected by LC-MS (SI Figs. S15 and S16) and a potential RhB degradation transformation mechanism was proposed (Fig. 4a). The degradation process of RhB include deethylation, cleavage of chromophores, opening of ring and mineralization. Note that some phenols such as p-chlorophenol (4-CP) were produced during the degradation process. These phenols may continue to induce the degradation in basic conditions without irradiating because phenols can also react with PS under basic conditions [16]. This reaction could be attributed to the Elbs oxidation reaction, which reported by Elbs in 1893 [34]. The o-nitrophenol can be oxidized to nitroquinol by the action of ammonium persulfate under alkali condition. Thereafter, the reaction has been extended to include a large amount of phenols [35,36]. Therefore, the effects of these substance on PS activation should be investigated. As shown in Fig. 4b, the RhB degradation was first carried out under visible light illuminating. After 15 min photoreaction, RhB and PS concentration decreased from 10 mg/L and 0.65 μM to approximately 5 mg/L and 0.4 μM, respectively. When the light was turned off, no obvious degradation of RhB can be observed. However, RhB concentration further decreased to 3.2 mg/L with the addition of NaOH. When the same concentration of NaOH and PS was added to the newly preparative 5 mg/L RhB solution, the concentration of RhB was only reduced to 4.5 mg/L (SI Fig. S17). This result indicated that the PS activation by base is weak and that these phenols can further activate PS under basic conditions. To further identify the role of these phenols, 4-CP was used to probe PS activation behavior. In the presence of 4-CP, the intensity of 7-HC obvious enhanced at pH 12 (SI Fig. S18), indicating that 4-CP can activate PS to produce radicals, which is consistent with previous research [16]. Since PS can be activated by phenols to generate free radicals, the mineralization efficiency can be further improved by base treatment. As shown in Fig. 4c, TOC removal efficiency was 20% in RhB/PS/Vis system within 60 min. Interestingly, TOC removal efficiency reached up to 32% after treatment by base for 120 min in the dark. The results demonstrated that simple base treatment can further improve the mineralization efficiency of the system due to the PS activation by phenoxide [16] and base [12]. It should be mentioned that only the anionic form of phenols could activate PS, thus an basic pH environment is necessary.

3.5. Wastewater treatment by photoexcited dye-activated PS

3.5.1. Simulation wastewater treatment

To probe whether photoexcited dye can be used as PS activator for treatment of complex wastewater, the effects of photoexcited RhB on the degradation of 10 mg/L TC-H or 2,4-DNP by PS were investigated. Fig. 5a showed 50.1% of 2,4-DNP was degraded in RhB/PS/Vis system, while only 12% and 13% of 2,4-DNP was degraded in PS/Vis system and RhB/Vis system, respectively. Similarly, the degradation of TC-H was distinct enhanced in the presence of RhB (Fig. 5b). The result demonstrated that RhB could act as the PS activator for the removal of environmental contaminants. It should mention that TC-H was degraded even in the absence of RhB due to the direct photolysis caused by its relatively unstable structure. Above results demonstrated that the concept of using dyes with PS and visible light to treat complex wastewater could be useful in those cases, where dyes are presented as wastewaters constituents. A similar idea has been proposed by J. Bolobajev et al. where they demonstrated tannic acid as wastewater constituent participation in the Fenton reaction and improved Fenton-based oxidation of contaminants in water [37].

3.5.2. Practical scenario application

Additionally, to explore the more practical scenario, using RhB as the PS activator for TC-H degradation under natural sunlight irradiation was studied. Under sunlight irradiation, the removal efficiency of TC-H by PS was significantly enhanced in the presence of RhB (Fig. 5c). During the daytime (11:00 a.m. to16:00p.m.), about 70% of TC-H was degraded by PS in the presence of RhB, while only 28% of TC-H was degraded by PS alone. This result revealed that RhB could act as an efficient PS activator under sunlight irradiation for environment purification. Given that the high energetic costs of UV-based AOPs, sunlight-activated PS activation could further save energy and ensure sustainable treatment.

3.6. Mechanism of pollutant degradation by photoexcited dye-activated PS

It has been demonstrated that photoexcited dyes can activate PS to generate radicals (Figs. 2 and 3). However, the reaction might become more complicated in the presence of other organic pollutants, such as TC-H. It is necessary to see if there are other reaction besides the free radical reaction. RhB can absorb light to produce photoexcited electrons and RhB^{*+} (Eq. (2)). Since the photoexcited electrons were mainly related to the generation of radicals, the role of RhB^{*+} also need to be identified. For this purpose, $KBrO_3$ was used to quench the photoexcited electrons in TC-H/RhB/Vis system and the concentration of TC-H and RhB were monitored (SI Fig. S19a). It can be observed that the concentration of RhB had no obvious change, while the concentration of TC-H were gradually decreased, indicating that the degradation of TC-H was occurred. It should mention that $KBrO_3$ itself couldn't cause the degradation of TC-H (SI Fig. S19b). Since the photoexcited electrons were removed by $KBrO_3$, the observed the degradation of TC-H might be origin from the direct electron transfer from TC-H to RhB^{*+}, which was a non-radical pathway (SI Fig. S20). This process was performed by direct electron transfer and did not involve the generation of radicals. Photoexcited electrons was consumed by electron acceptor and RhB^{*+} with a certain oxidizing ability can direct withdraw the electrons from TC-H. In RhB/TC-H/PS/Vis system, on the one hand, PS can be activated by photoexcited electrons to produce radicals. On the other hand, it act as the electron acceptor to mediated the non-radical pathway. (SI Fig. S21) ROSs quenching experiments further confirmed that free radicals were main ROSs, but excess EtOH could not completely inhibit the degradation of TC-H (SI Fig. S22), suggesting the presence of non-radical reactions. Therefore, the degradation of TC-H in RhB/PS/Vis involved both radical and non-radical reaction pathway, where the radical reaction pathway was the major route. The detailed mechanism was displayed in Fig. 6.

4. Conclusion

This study demonstrated that dyes showed autocatalysis degradation under visible light irradiation due to the PS activation by dye itself. Both radical and nonradical reaction occurred when using dye as the PS activator for degradation of organic pollutants such as TC-H. Photoexcited electrons mainly induce the generation of radicals, while RhB^{*+} could directly withdraw the electrons from TC-H.

RhB as the activator also can be degradation by radicals. Once the RhB was degraded completely, the PS activation will stop. Interestingly, the phenol intermediates of RhB degradation can further activate PS to produce radicals in base conditions. Thus, the residual by-product can be removed easily by simple post-processing with base.

The activation of PS by dye was influenced by the type of dye, dose of dye, and pH. Due to the electrostatic repulsion between the anion dye and PS, its activation efficiency toward PS is inferior to that of cationic dye. The activation of PS by RhB was inhibited as the pH values increase due to the weaker electrostatic attraction between the deprotonation RhB and PS.

This catalyst-free AOPs not only save costs but also avoid secondary pollution. Especially, it can also be operated under natural sunlight irradiation, which further save energy compared with UV-based AOPs. Additionally, This strategy not only can alleviate the burden of dye wastewater disposal, but also achieved a "using waste to treat waste" goal.

Acknowledgements

This work was supported by the National Natural Science Foundation of China (51872089, 51478171 and 51672077), Hunan Provincial Natural Science Foundation of China (2017JJ2026), Youth Natural Science Foundation of Hunan Province (Nos. 2019JJ50044) and China Postdoctoral Science Foundation. (Nos. 2018M632956, 2019T120710).

Appendix A. Supplementary data

Supplementary data to this article can be found online at https://doi.org/10.1016/j.cej.2019.122070.

References

[1] L. Yang, Z. Chen, D. Cui, X. Luo, B. Liang, L. Yang, T. Liu, A. Wang, S. Luo, Ultrafine palladium nanoparticles supported on 3D self-supported Ni foam for cathodic dechlorination of florfenicol, Chem. Eng. J. 359 (2019) 894–901.
[2] S. Wacławek, H.V. Lutze, K. Grübel, V.V.T. Padil, M. Černík, D.D. Dionysiou, Chemistry of persulfates in water and wastewater treatment: a review, Chem. Eng. J. 330 (2017) 44–62.
[3] X. Duan, H. Sun, J. Kang, Y. Wang, S. Indrawirawan, S. Wang, Insights into heterogeneous catalysis of persulfate activation on dimensional-structured nanocarbons, ACS Catal. 5 (2015) 4629–4636.
[4] P. Hu, H. Su, Z. Chen, C. Yu, Q. Li, B. Zhou, P.J.J. Alvarez, M. Long, Selective degradation of organic pollutants using an efficient metal-free catalyst derived from carbonized polypyrrole via peroxymonosulfate activation, Environ. Sci. Technol. 51 (2017) 11288–11296.
[5] H. Li, C. Shan, B. Pan, Fe(III)-Doped g-C_3N_4 mediated peroxymonosulfate activation for selective degradation of phenolic compounds via high-valent iron-oxo species, Environ. Sci. Technol. 52 (2018) 2197–2205.
[6] G. Fang, J. Gao, D.D. Dionysiou, C. Liu, D. Zhou, Activation of persulfate by quinones: free radical reactions and implication for the degradation of PCBs, Environ. Sci. Technol. 47 (2013) 4605–4611.
[7] P. Hu, M. Long, Cobalt-catalyzed sulfate radical-based advanced oxidation: a review on heterogeneous catalysts and applications, Appl. Catal., B 181 (2016) 103–117.
[8] G.P. Anipsitakis, D.D. Dionysiou, Radical generation by the interaction of transition metals with common oxidants, Environ. Sci. Technol. 38 (2004) 3705–3712.
[9] T. Zhang, Y. Chen, Y. Wang, J. Le Roux, Y. Yang, J.P. Croue, Efficient peroxydisulfate activation process not relying on sulfate radical generation for water pollutant degradation, Environ. Sci. Technol. 48 (2014) 5868–5875.
[10] T. Zhang, H. Zhu, J.-P. Croue, Production of sulfate radical from peroxymonosulfate induced by a magnetically separable $CuFe_2O_4$ spinel in water: efficiency, stability, and mechanism, Environ. Sci. Technol. 47 (2013) 2784–2791.
[11] X. Cheng, H. Guo, Y. Zhang, X. Wu, Y. Liu, Non-photochemical production of singlet oxygen via activation of persulfate by carbon nanotubes, Water Res. 113 (2017)

80–88.
[12] Y. Zhou, Y. Xiang, Y. He, Y. Yang, J. Zhang, L. Luo, H. Peng, C. Dai, F. Zhu, L. Tang, Applications and factors influencing of the persulfate-based advanced oxidation processes for the remediation of groundwater and soil contaminated with organic compounds, J. Hazard. Mater. 359 (2018) 396–407.
[13] C. Luo, J. Ma, J. Jiang, Y. Liu, Y. Song, Y. Yang, Y. Guan, D. Wu, Simulation and comparative study on the oxidation kinetics of atrazine by UV/H_2O_2, UV/HSO_5^- and UV/$S_2O_8^{2-}$, Water Res. 80 (2015) 99–108.
[14] P. Xie, J. Ma, W. Liu, J. Zou, S. Yue, X. Li, M.R. Wiesner, J. Fang, Removal of 2-MIB and geosmin using UV/persulfate: contributions of hydroxyl and sulfate radicals, Water Res. 69 (2015) 223–233.
[15] Y. Zhou, J. Jiang, Y. Gao, J. Ma, S.Y. Pang, J. Li, X.T. Lu, L.P. Yuan, Activation of peroxymonosulfate by benzoquinone: a novel nonradical oxidation process, Environ. Sci. Technol. 49 (2015) 12941–12950.
[16] M. Ahmad, A.L. Teel, R.J. Watts, Mechanism of persulfate activation by phenols, Environ. Sci. Technol. 47 (2013) 5864–5871.
[17] Y. Zhou, J. Jiang, Y. Gao, S.Y. Pang, Y. Yang, J. Ma, J. Gu, J. Li, Z. Wang, L.H. Wang, L.P. Yuan, Y. Yang, Activation of peroxymonosulfate by phenols: important role of quinone intermediates and involvement of singlet oxygen, Water Res. 125 (2017) 209–218.
[18] S.S. Lee, H. Bai, Z. Liu, D.D. Sun, Novel-structured electrospun TiO_2/CuO composite nanofibers for high efficient photocatalytic cogeneration of clean water and energy from dye wastewater, Water Res. 47 (2013) 4059–4073.
[19] W. Chu, Dye removal from textile dye wastewater using recycled alum sludge, Water Res. 35 (2001) 3147–3152.
[20] A. Mishra, M.K. Fischer, P. Bauerle, Metal-free organic dyes for dye-sensitized solar cells: from structure: property relationships to design rules, Angew. Chem. Int. Ed. Engl. 48 (2009) 2474–2499.
[21] Y. Ooyama, S. Inoue, T. Nagano, K. Kushimoto, J. Ohshita, I. Imae, K. Komaguchi, Y. Harima, Dye-sensitized solar cells based on donor-acceptor pi-conjugated fluorescent dyes with a pyridine ring as an electron-withdrawing anchoring group, Angew. Chem. Int. Ed. Engl. 50 (2011) 7429–7433.
[22] Y. Gao, Z. Zhang, S. Li, J. Liu, L. Yao, Y. Li, H. Zhang, Insights into the mechanism of heterogeneous activation of persulfate with a clay/iron-based catalyst under visible LED light irradiation, Appl. Catal., B 185 (2016) 22–30.
[23] C. Marsh, J.O. Edwards, The free-radical decomposition of peroxymonosulfate, Prog. React. Kinet. 15 (1989) 35–75.
[24] S. Srisantitham, M. Sukwattanasinitt, S. Unarunotai, Effect of pH on fluorescence quenching of organic dyes by graphene oxide, Colloids Surface A 550 (2018) 123–131.
[25] K.-I. Ishibashi, A. Fujishima, T. Watanabe, K. Hashimoto, Detection of active oxidative species in TiO_2 photocatalysis using the fluorescence technique, Electrochem. Commun. 2 (2000) 207–210.
[26] H. Li, C. Shan, W. Li, B. Pan, Peroxymonosulfate activation by iron(III)-tetraamidomacrocyclic ligand for degradation of organic pollutants via high-valent iron-oxo complex, Water Res. 147 (2018) 233–241.
[27] Y. Yang, G. Banerjee, G.W. Brudvig, J.H. Kim, J.J. Pignatello, Oxidation of organic compounds in water by unactivated peroxymonosulfate, Environ. Sci. Technol. 52 (2018) 5911–5919.
[28] Y. Gao, Y. Zhu, L. Lyu, Q. Zeng, X. Xing, C. Hu, Electronic structure modulation of graphitic carbon nitride by oxygen doping for enhanced catalytic degradation of organic pollutants through peroxymonosulfate activation, Environ. Sci. Technol. 52 (2018) 14371–14380.
[29] A. Syoufian, K. Nakashima, Degradation of methylene blue in aqueous dispersion of hollow titania photocatalyst: study of reaction enhancement by various electron scavengers, J. Colloids Interface Sci. 317 (2008) 507–512.
[30] C. Alexopoulou, A. Petala, Z. Frontistis, C. Drivas, S. Kennou, D.I. Kondarides, D. Mantzavinos, Copper phosphide and persulfate salt: a novel catalytic system for the degradation of aqueous phase micro-contaminants, Appl. Catal., B 244 (2018) 178–187.
[31] S. Zhang, L. Wang, C. Liu, J. Luo, J. Crittenden, X. Liu, T. Cai, J. Yuan, Y. Pei, Y. Liu, Photocatalytic wastewater purification with simultaneous hydrogen production using MoS_2 QD-decorated hierarchical assembly of $ZnIn_2S_4$ on reduced graphene oxide photocatalyst, Water Res. 121 (2017) 11–19.
[32] E. Haque, J.W. Jun, S.H. Jhung, Adsorptive removal of methyl orange and methylene blue from aqueous solution with a metal-organic framework material, iron terephthalate (MOF-235), J. Hazard. Mater. 185 (2011) 507–511.
[33] T.A. Saleh, V.K. Gupta, Functionalization of tungsten oxide into MWCNT and its application for sunlight-induced degradation of rhodamine B, J. Colloids Interface Sci. 362 (2011) 337–344.
[34] S.M. Sethna, The elbs persulfate oxidation, Chem. Rev. 49 (1951) 91–101.
[35] E.J. Behrman, P.P. Walker, The elbs peroxydisulfate oxidation: kinetics, J. Am. Chem. Soc. 84 (1962) 3454–3457.
[36] E.J. Behrman, Peroxydisulfate chemistry in the environmental literature: a brief critique, J. Hazard. Mater. 365 (2019) 971.
[37] J. Bolobajev, M. Trapido, A. Goi, Interaction of tannic acid with ferric iron to assist 2,4,6-trichlorophenol catalytic decomposition and reuse of ferric sludge as a source of iron catalyst in Fenton-based treatment, Appl. Catal., B 187 (2016) 75–82.